ELSEVIER

Journal of Luminescence 64 (1995) 189-193

JOURNAL OF LUMINESCENCE

The $^5D_2 \rightarrow {}^7F_0$ transition probability and its effect on hole-burning quantum efficiency in $BaFCl_xBr_{1-x}:Sm^{2+}$

Hongwei Song*, Jiahua Zhang, Shihua Huang, Jiaqi Yu

Laboratory of Excited State Process, Changchun Institute of Physics, Academia Sinica, Changchun 130021, China

Received 29 August 1994; revised 22 November 1994; accepted 13 December 1994

Abstract

In this paper, The $^5D_2 \rightarrow {}^7F_0$ emission transition probability in $BaFCl_xBr_{1-x}:Sm^{2+}$ system was studied. The experimental studies show that, with the increase of Br concentration in the $BaFCl_xBr_{1-x}:Sm^{2+}$ system, the 4f5d bands of Sm^{2+} are nearer to the $^5D_2$ level and the $^5D_2 \rightarrow {}^7F_0$ transition probabilities increase. The effect of the $^5D_2 \rightarrow {}^7F_0$ transition probability on the hole-burning quantum efficiency is analyzed. The increase of $^5D_2 \rightarrow {}^7F_0$ transition probability favours the increase of the hole-burning quantum efficiency.

1. Introduction

Materials of the $M_yM'_{1-y}FCl_xBr_{1-x}:Sm^{2+}$ series (M = Mg, Ca, Sr, Ba) have been widely studied in photon-gated spectral hole-burning studies since the first observation of the spectral hole burning in $BaFCl:Sm^{2+}$ at 2 K was reported by Winnaker et al. in 1985 [1]. Then, the hole-burning in the Sm^{2+} mixed crystals at 77 K [2-4] and room temperature [5-7] has been reported, respectively. The spectral hole burning of Sm^{2+} in fluorohafnate glasses [8,9] at room temperature has also been reported in recent years. These materials have potential use in high temperature hole-burning for optical information storage.

Hole burning in $BaFCl_xBr_{1-x}:Sm^{2+}$ system can be performed in the $^7F_0 \rightarrow {}^5D_J$ ($J = 0, 1, 2$) transitions (See Fig. 1). Because the $^7F_0 \rightarrow {}^5D_J$ transition is a $4f^6$–$4f^6$ electric-dipole-parity forbidden transition, it has a small absorption cross section and low hole-burning quantum efficiency. So it is important to increase the $^7F_0 \rightarrow {}^5D_J$ transition probability and thus to increase hole-burning quantum efficiency which is the main obstacle for these materials to have practical use in optical information storage.

The increase of $^5D_2 \rightarrow {}^7F_0$ favours the increase of the quantum hole-burning efficiency.

2. Experimental

The samples were prepared by the same method as described in Ref. [2]. The nominal molar concentration of Sm_2O_3 is 0.5%. $BaFCl_xBr_{1-x}:Sm^{2+}$ samples were prepared with different values of x (x = 1.0, 0.75, 0.5, 0.25, 0).

Excitation spectra of $BaFCl_xBr_{1-x}:Sm^{2+}$ were measured by monitoring the $^5D_0 \rightarrow {}^7F_0$ emission

---

* Corresponding author.

SSDI 0022-2313(95)00030-5

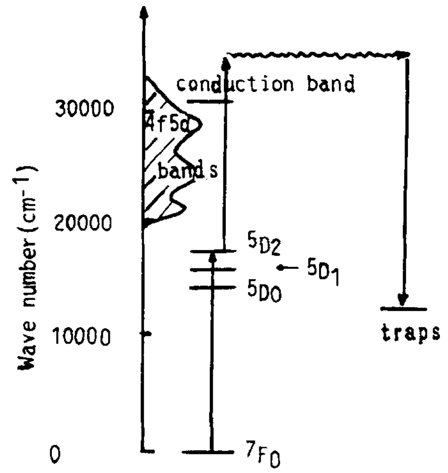

Fig. 1. Schematic diagram of hole-burning in $BaFCl_xBr_{1-x}:Sm^{2+}$.

Fig. 2. Excitation spectra of $BaFCl_xBr_{1-x}:Sm^{2+}$ measured by monitoring $^5D_0 \rightarrow {}^7F_0$ emission and scanning the range of 4f5d bands. (a) $x = 0$; (b) $x = 0.25$; (c) $x = 0.5$; (d) $x = 0.75$; (e) $x = 1.0$.

and scanning the range of the 4f5d bands with a Hitachi F-4000 spectrometer. In the process of measuring the fluorescence spectra and the fluorescence decays, the samples were pumped by a nitrogen laser and contained within a helium gas closed-cycling cryostat or immersed into liquid nitrogen. A D330 Monochromater, a Boxcar averager and a Datemate microcomputer were used to detect and analyze the fluorescence of $BaFCl_xBr_{1-x}$: Sm^{2+} samples.

3. Results and discussion

3.1. *The 4f5d bands positions of the samples with different x*

Fig. 2 shows the 4f5d bands in the excitation spectra of $BaFCl_xBr_{1-x}:Sm^{2+}$. We can see that there are four peaks in each 4f5d bands. The peak which is nearest to $^5D_2$ energy level is at about 480 nm and there is a shoulder on the low energy side of the peak. The smaller the value of x, the lower the energy of the shoulder, the energy separation between the 480 nm peak and the shoulder is from several nm to more than 10 nm for the samples with different x. On the other hand, the positions of $^5D_2$ energy level is almost unchanged with x, therefore Fig. 2 shows that the position of the 4f5d bands is nearer to the $^5D_2$ energy level with decreasing x.

The f–f transitions of rare earth ions are first order electric-dipole-parity forbidden transitions. But it is well known that most of the transitions of rare earth ion are electric-dipole transitions. In the light of the Judd–Ofelt theory [10, 11], the reason is that the opposite-parity states are mixed into $4f^n$ states by odd parity static or dynamic crystal field. In $BaFCl_xBr_{1-x}:Sm^{2+}$, the $^5D_2$ level is very near the 4f5d bands which have opposite parity, mixing of wave functions becomes significant.

If $|\Psi' J' J_z'\rangle$ is the wave function of the $^5D_2$ energy level and $|\Psi''\rangle$ is the wave function of the 4f5d bands, the mixed state $|B\rangle$ of the $^5D_2$ energy level is as follows:

$$|B\rangle = |\Psi' J' J'_z\rangle + \sum_{''} \frac{|\Psi''\rangle\langle\Psi''|H_c|\Psi' J' J_z'\rangle}{E(\Psi' J' J_z') - E(\Psi'')},$$

where H_c is Hamiltonian of interaction to produce mixture of wave functions. If $\langle A| = \langle \Psi' J' J_z'|$ is a state of $^7F_0$, the matrix elements of electric dipole P are as below:

$$\langle A|P|B\rangle = \sum_{\Psi''} \frac{\langle \Psi J J_z|P|\Psi''\rangle\langle \Psi''|H_c|\Psi' J' J_z'\rangle}{E(\Psi' J' J_z') - E(\Psi'')},$$

since $|\Psi''\rangle$ is the state of the 4f5d bands, $\langle \Psi J J_z|P|\Psi''\rangle$ is a parity allowed matrix element. The smaller the energy separation $[E('J'J_z') - E(\psi'')]$, the larger the value of the $^5D_2 \rightarrow {}^7F_0$ transition probability. So it is expected that the $^5D_2 \rightarrow {}^7F_0$ radiative transition probability increases with the decrease of x. This is consistent with the experimental results in Section 3.2.

3.2. Dependence of the $^5D_2 \rightarrow {}^7F_0$ electron transition probability on the value of x

In our experiments, it is found that the $^5D_2 \rightarrow {}^7F_0$ fluorescence changed with the approach of the 4f5d bands to the $^5D_2$ level. Firstly, the $^5D_2 \rightarrow {}^7F_0$ fluorescence decay time decreased (see Fig. 3). Secondly, the intensity ratio of the $^5D_2 \rightarrow {}^7F_0$ to the $^5D_1 \rightarrow {}^7F_0$ transition at 77 K decreased with the decrease of x (see Fig. 4).

Fig. 3 shows the dependence of the $^5D_2 \rightarrow {}^7F_0$ fluorescence decays on temperature. From Fig. 3 we see that, at temperature below 30 K, the $^5D_2 \rightarrow {}^7F_0$ emission decay times approach saturation values. With the increase of temperature, the $^5D_2 \rightarrow {}^7F_0$ decay times are shortened and the $^5D_2 \rightarrow {}^7F_0$ intensities become weaker, so that at 100 K temperature, the $^5D_2 \rightarrow {}^7F_0$ fluorescence is difficult to be detected. The nonradiative transition probability decrease with decrease of temperature. It is well known that decay time $\tau = 1/(R + W_{nr})$, where R and W_{nr} are the radiative and nonradiative transition probability, respectively. At low temperature, τ approaches $1/R$, which is a saturation value of τ. At temperature below 30 K, the $^5D_2 \rightarrow {}^7F_0$ decay times approach saturation values. This means that the nonradiative transition probabilities below 30 K are negligible comparing with the radiative transition probabilities [13]. In that case, the $^5D_2 \rightarrow {}^7F_0$ decay times were determined by the radiative transition probabilities of $^5D_2$. So the $^5D_2 \rightarrow \Sigma_J {}^7F_J$ radiative transition probabilities equal $1/\tau_0$ (τ_0 is the saturation value of the $^5D_2 \rightarrow {}^7F_0$ decay time. By this method, we get the dependence of the $^5D_2 \rightarrow \Sigma_J {}^7F_J$ radiative

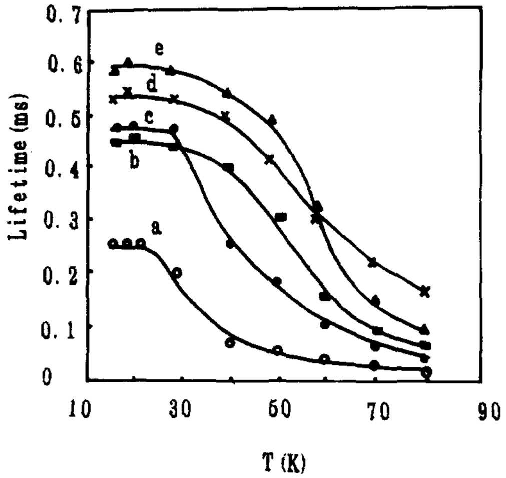

Fig. 3. Dependence of the $^5D_2 \rightarrow {}^7F_0$ fluorescence decays in $BaFCl_xBr_{1-x}$: Sm^{2+} series with different values of x on temperature. (a) $x = 0$; (b) $x = 0.25$; (c) $x = 0.5$; (d) $x = 0.75$; (e) $x = 1.0$.

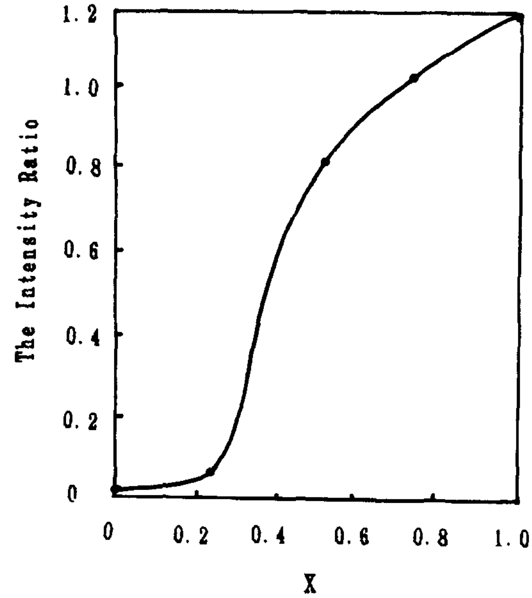

Fig. 4. Dependence of the fluorescence intensity ratio of $^5D_2 \rightarrow {}^7F_0$ to $^5D_1 \rightarrow {}^7F_0$ transition on values of x at 77 K.

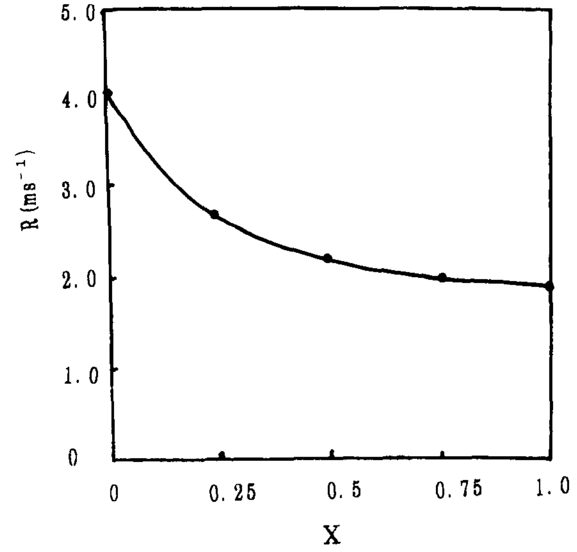

Fig. 5. Dependence of the $^5D_2 \rightarrow \Sigma_J\ ^7F_J$ transition probability in BaFCl$_x$ Br$_{1-x}$:Sm^{2+} series on values of x.

transition probability R on value of x (see Fig. 5). The $^5D_2 \rightarrow \Sigma_J\ ^7F_J$ radiative transition probability increases with decrease of x. This result is attributed to increase of each $^5D_2 \rightarrow {}^7F_J$ transition. According to experimental results, the relative intensity of each $^5D_2 \rightarrow {}^7F_J$ almost does not change with x. So the $^5D_2 \rightarrow {}^7F_0$ transition probability is proportional to the $^5D_2 \rightarrow \Sigma_J\ ^7F_J$ radiative transition probability. The $^5D_2 \rightarrow {}^7F_0$ transition probability increases with increase of Br concentration.

According to the Einstein equation:

$$R' = 8\pi h \nu^3 R/c^3,$$

where R' is the absorption probability. We can obtain the $^7F_0 \rightarrow {}^5D_2$ absorption probability which is a important parameter for hole-burning efficiency.

The nonradiative transitions of $^5D_2$ include the $^5D_2 \rightarrow$ 4f5d electron thermal activation and the $^5D_2 \rightarrow {}^5D_1$ multi-phonon relaxation. The $^5D_2 \rightarrow$ 4f5d electron thermal activation is a strong-coupling interaction and the $^5D_2 \rightarrow {}^5D_1$ electron nonradiative relaxation is a weak-coupling interaction. In the light of the theory of multi-phonon relaxation [12]:

$$W_1 = W_{10}e^{-\Delta E_1/KT},$$

$$W_2 = W_{20}e^{-\Delta E_2/KT}(1 + \langle n \rangle)^p,$$

where, W_1 is the $^5D_2 \rightarrow$ 4f5d electron thermal activation probability and W_2 is the $^5D_2 \rightarrow {}^5D_1$ multi-phonon relaxation probability. ΔE_1 and ΔE_2 are energy difference between $^5D_2$ and 4f5d bands and that between $^5D_2$ and $^5D_1$ respectively. $\langle n \rangle = e^{-\hbar\omega/kT}/(1 - e^{-\hbar\omega/kT})$ is the average population of phonons.

Based on the above formulation, the smaller the value of x, the smaller the energy interval of the $^5D_2$ level and the 4f5d bands, the larger the $^5D_2 \rightarrow {}^7F_0$ electron thermal activation probability W_1. We know from the experimental results that change of x has little effect on ΔE_2. We assume that change of x does not effect W_2 strongly. Sum up the above discussion, the increase of the $^5D_2$ electron radiative and nonradiative transition probabilities with decrease of x makes the $^5D_2 \rightarrow {}^7D_2$ fluorescence decay times shortened and the intensity ratio of $^5D_2 \rightarrow {}^7F_0$ to $^5D_1 \rightarrow {}^7F_0$ transition decreased.

3.3. *The effect of the $^5D_2 \rightarrow {}^7F_0$ absorption probability on hole-burning quantum efficiency*

For the hole-burning experiment in the $^5D_2 \rightarrow {}^7F_0$ transition with pulsed laser, an approximate solution was derived as follows [14] in the light of the dynamical equations of the three energy level system:

$$N_3 = \eta_{23} II' \sigma_0 \sigma_1 \mu \tau' N_0\, e^{-anT},$$

where, N_3 is the number of electrons captured by traps in the nth pulse. η_{23} is the probability that traps capture electrons from conduction band, there η_{23} is taken as a constant. I and I' are the intensities of hole-burning laser and the gating laser, σ_0 and σ_1 are the $^7F_0 \rightarrow {}^5D_2$ and the $^5D_2 \rightarrow$ 4f5d absorption cross sections respectively, μ is the pulse width of the laser pulse. τ' is the electron lifetime of the conduction band, N_0 is the $^7F_0$ electron populations, $a = \ln[(1 - \eta_{23} I I' \sigma_0 \sigma_1 \mu \tau' N_0)/T]$, $n = 0, 1, 2, \ldots, T$ is the interval of the laser pulses.

The hole-burning quantum efficiency η is defined as the number of trapped electrons produced by a hole-burning photon when t approaches 0, so there is:

$$\eta = N_3\, h\omega / I\mu = \eta_{23}\, \sigma_0\, \sigma_1\, I'\tau' N_0\, h\omega .$$

Since σ_0 is proportional to the absorption probability R' of $^7F_0 \rightarrow {}^5D_2$, so the hole-burning quantum efficiency η is proportional to R'.

Therefore, in the case of weak excitation pumped and gated by a pulsed laser, since the $^7F_0 \rightarrow {}^5D_2$ absorption probability of $BaFCl_xBr_{1-x}:Sm^{2+}$ increases with decrease of x, the hole-burning quantum efficiency performed in $^5D_2$ energy level is expected to be enhanced with the increase of Br concentration.

4. Conclusions

In $BaFCl_xBr_{1-x}:Sm^{2+}$ system, the higher the concentration of Br, the nearer the $^5D_2$ level and 4f5d bands, the larger the $^7F_0 \rightarrow {}^5D_2$ absorption probability. In the process of the hole burning pumped and gated by a pulsed laser, the hole-burning quantum efficiency is proportional to the $^7F_0 \rightarrow {}^5D_2$ absorption probability R'. It is possible to enhance the $^7F_0 \rightarrow {}^5D_2$ hole-burning quantum efficiency with the increase of Br concentration.

References

[1] A. Winnaker, R. M. Shelby, R. M. Macfarlane, Opt. Lett. 10 (1985) 350.

[2] Changjiang Wei, Shihua Huang, Jiaqi Yu, J. Lumin. 43 (1989) 161.

[3] Jiahua Zhang, Shihua Huang, Weiqing Qin, Diankun Gao, Jiaqi Yu, J. Lumin. 53 (1992) 275.

[4] Changjiang Wei, Alredj. Meixner, Mawro. Croci, Urs. P. Wild, J. Lumin. 53 (1992).

[5] Jiahua Zhang, Shihua Huang, Jiaqi Yu, Chinese J. Lumin. 12 (1991) 181

[6] Keith Holloday, Changjiang Wei, Mawro Croci, Urs. P. Wild, J. Lumin. 53 (1992) 227.

[7] Jia hua Zhang, Shihua Huang, Jiaqi Yu, Opt. Lett. 17 (1992) 149.

[8] R. Jaaniso, H. Bill. Euro, Phys. Lett. 16 (1991) 569.

[9] K. Hirao, S. Todoroki, N. Soga, J. Lumin. 55 (1993) 217.

[10] B. R. Judd, Phys. Rev. 127 (1962) 719.

[11] G. R. Ofelt, J. Chem. Phys. 37 (1962) 511.

[12] T. M. Yakawa, D. L. Dexter, Phys. Rev. B 1 (1970) 2961.

[13] Hongwei Song, Jiahua Zhang, Shihua huang, Jiaqi Yu, Chinese J. Lumin 3 (1994) 215.

[14] Hongwei Song, Jiahua Zhang, Shihua huang, Jiaqi Yu, Chinese J. Lumin. 3 (1994) 201.